Journal of Cosmology and
Astroparticle Physics

PAPER

Ultra-peripheral collisions of charged hadrons in extensive air showers

To cite this article: Manuel Masip *et al* JCAP07(2023)025

Journal of Cosmology and Astroparticle Physics
An IOP and SISSA journal

Ultra-peripheral collisions of charged hadrons in extensive air showers

Manuel Masip,[a] Ivan Rosario[a] and Sergio J. Sciutto[b]

[a]CAFPE and Departamento de Física Teórica y del Cosmos, Universidad de Granada, E-18071 Granada, Spain

[b]Departamento de Física e Instituto de Física La Plata (CONICET), Universidad Nacional de La Plata, C.C. 69 (1900) La Plata, Argentina

E-mail: masip@ugr.es, ivan.rosario@ugr.es, sciutto@fisica.unlp.edu.ar

Received March 31, 2023
Accepted June 21, 2023
Published July 11, 2023

Abstract. We discuss the electromagnetic collisions of high energy protons, pions and kaons with atmospheric nuclei. In particular, we use the equivalent photon approximation to estimate *(i)* the diffractive collisions where the projectile scatters inelastically off a nucleus, and *(ii)* the usual radiative processes (bremsstrahlung, pair production and photonuclear interactions) of these charged hadrons in the air. We then include the processes in the simulator AIRES and study how they affect the longitudinal development of extensive air showers. For 10^{9-11} GeV proton primaries we find that they introduce a very small reduction (below 1%) in the average value of both $X_{\rm max}$ and $\Delta X_{\rm max}$. At a given shower age (relative slant depth from $X_{\rm max}$), these electromagnetic processes slightly increase the number of charged particles at the shower maximum and reduce the number of muons when it is old, decreasing by 1% the muon-to-$(\gamma + e)$ near the ground level.

Keywords: cosmic ray theory, ultra high energy cosmic rays

ArXiv ePrint: 2303.16042

 https://doi.org/10.1088/1475-7516/2023/07/025

Contents

1 Introduction 1

2 Bremsstrahlung and diffractive collisions 3

3 Pair production and photonuclear collisions 5

4 AIRES simulations 7

5 Summary and discussion 12

1 Introduction

Cosmic rays (CRs), with energies of up to 10^{11} GeV, provide a window for the exploration of collisions at extreme energies. When they reach the Earth, the atmosphere acts like a calorimeter of very low density but equivalent to 10 m of water,[1] resulting in an extensive air shower (EAS) that includes three basic components: a hadronic one, an electromagnetic (EM) one with photons and electrons, plus a component with muons and neutrinos from light meson decays [1, 2]. Fluorescence and surface detectors at observatories like AUGER [3] can then estimate the total energy of the primary, the atmospheric depth $X_{\rm max}$ with the maximum number of charged particles, and the number and distribution of electrons and muons reaching the ground. The relation of these observables with the spectrum and composition of the primary CR flux faces an obvious difficulty: since we do not have access to a controlled source of CRs, this atmospheric calorimeter can not be properly calibrated, and the results will heavily rely on Monte Carlo simulations.

It then becomes essential to identify all the relevant processes in the EAS and the main sources of uncertainty in the simulations [4]. In particular, CR collisions involve a high energy regime[2] and a kinematical region (ultraforward rapidities are critical in the longitudinal development of a shower) that are of difficult access at colliders. Moreover, lower energy processes may introduce corrections that, given the large number of collisions in the core of an EAS before it reaches the ground, may become sizeable. For example, most of the EM energy in the shower is generated through π^0 decays high in the atmosphere. As this energy goes forward it degrades after each radiation length ($X_0 \approx 38\text{g/cm}^2$). Since the cross section for a hadronic collision of a photon with an air nucleus is 100 times smaller, this degradation happens mostly through purely EM processes ($\gamma A \to e^+e^- A$ and $eA \to e\gamma A$). This initial EM energy, however, crosses a large depth before it is absorbed (e.g., it takes around 20 radiation lengths to reduce a 10^6 GeV photon to 1 GeV electrons and photons). As a consequence, the probability that part of the EM energy goes back to hadrons within that interval can not be ignored. This is illustrated in figure 1 for 10^{10} GeV proton showers. If the hadronic collisions of photons are turned off in AIRES [5], we find an 8.3% reduction in the average number of muons from meson decays at the ground level.

[1] Or 20 m.w.e. if the primary enters from a zenith inclination $\theta_z = 60^\circ$.

[2] Notice that a 10^8 GeV proton hitting an atmospheric nucleon reproduces the 14 TeV center of mass energy currently studied at the LHC.

JCAP07(2023)025

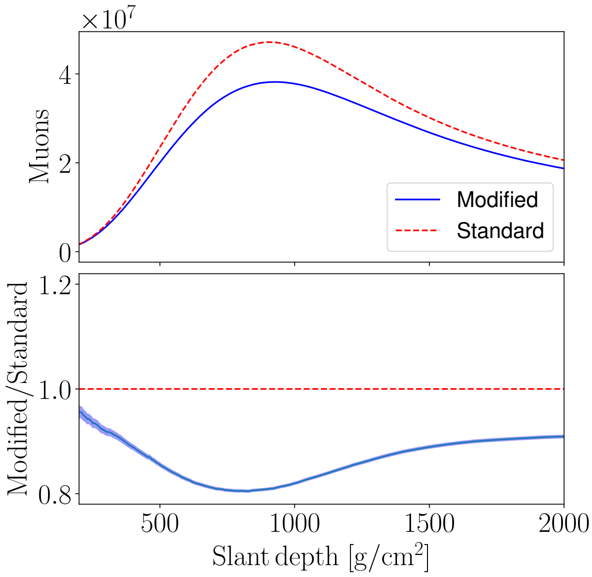

Figure 1. Muon content in the average 10^{10} GeV proton shower with (dashes) or without (solid) hadronic interactions of photons (from 40000 simulations with AIRES, $\theta_z = 70°$). The deficit (lower figure) goes from 20% at $X_{\rm max}$ to 8% at the surface.

Here we will discuss some effects that are neglected in current EAS simulators like AIRES or CORSIKA [6, 7]: the photon-mediated ultra-peripheral collisions of charged hadrons with atmospheric nuclei. A simple argument suggests that these processes should be taken into account. When one of these hadrons crosses the EM field of a nucleus it may get diffracted into a system of mass $m^* > m + m_\pi$ giving a final state with several hadrons, e.g.,

$$p\,A \to N\,\pi\,A\,. \tag{1.1}$$

Notice that at higher projectile energies, this inelastic process may occur at larger transverse distances: unlike the pomeron-mediated diffractive cross section, this one grows with the energy [8]. Its possible relevance may remind us to what happens in the propagation of CRs through the intergalactic medium, where the collisions with the CMB photons are irrelevant until they become inelastic at the GZK [9, 10] energy.

We will also discuss the radiative emissions of the charged hadrons in the atmosphere, namely, bremsstrahlung (BR), pair production (PP) and photonuclear (PN) collisions where the projectile is still present after the collision:

$$h\,A \to h\,\gamma\,A\,; \quad h\,A \to h\,e^+e^-A\,; \quad h\,A \to h\,\rho\,A \to h\,X\,, \tag{1.2}$$

with $h = p, K, \pi$. These processes are ultra-peripheral as well, at impact parameters $b > R_A$, with the EM field of h going into an e^+e^- pair (PP) or a ρ meson (PN) or with the projectile scattering off the EM field of the nucleus and emitting a photon (BR). We will use the equivalent photon approximation (EPA) to estimate the rate of all these processes and will discuss the validity of this approximation. Our objective is to obtain the precise effect of ultra-peripheral EM collisions in the longitudinal development of EASs.

2 Bremsstrahlung and diffractive collisions

A relativistic charged particle creates an EM field that can be approximated by a cloud of virtual photons [11]. These photons may interact with the photon cloud of another charged particle (in a $\gamma\gamma$ collision) or with the target particle itself. Notice that if the transverse distance between two charged hadrons in a collision is $b > R_1 + R_2$, these ultra-peripheral processes will not occur simultaneously with a hadronic one. For an atmospheric nitrogen nucleus N, the equivalent photons are coherently radiated, which imposes a limit on their minimum wavelength.

Let us be more specific. Consider a hadron h of energy E and mass m_h moving in the atmosphere. In its rest frame, h sees the nucleus N approaching with a Lorentz factor $\gamma = E/m_h$ and surrounded by the cloud of photons. In the transverse plane the photons have a momentum $p_T \leq 1/R_{\rm N} \approx 71\,{\rm MeV}$, whereas in the longitudinal direction their momentum can be much larger, $p_L \leq \gamma/R_{\rm N}$. The virtuality, $|q^2| < 1/R_N^2$, of these quasi-real photons is small compared to their energy. The total flux of equivalent photons around the nucleus is obtained with the Weizsaker-Williams method; upon integration in impact parameter space between $b_{\rm min}$ and $b_{\rm max}$ it gives [12]

$$\frac{{\rm d}N_\gamma}{{\rm d}\omega} = \frac{\alpha\, Z^2}{\pi\,\gamma^2}\left[\omega\, b^2\left(K_0(x)^2 - K_1(x)^2\right) + 2\gamma\, b K_1(x)\, K_0(x)\right]\Bigg|_{b_{\rm min}}^{b_{\rm max}}, \tag{2.1}$$

where ω is the energy of the photons, $K_n(x)$ modified Bessel functions of the second kind, $x = \omega b/\gamma$, $b_{\rm min} = R_{\rm N}$ and $b_{\rm max} \approx 1/(\alpha\, m_e)$. For the radius of a nucleus we will take $R_A = 5.8\, A^{1/3}\,{\rm GeV}^{-1}$.

It is then easy to describe the collision of this equivalent photon flux with a hadron h at rest. At low values of ω ($\omega \leq 1\,{\rm GeV}$) the dominant process is just Compton scattering; for $h = p$ the differential cross section reads

$$\frac{{\rm d}\sigma_{\gamma p\to\gamma p}}{{\rm d}\cos\theta} = \frac{\pi\alpha^2\,|F(t)|^2}{m_p^2}\left(\frac{\omega'}{\omega}\right)^2\left(\frac{\omega'}{\omega} + \frac{\omega}{\omega'} - 1 + \cos^2\theta\right), \tag{2.2}$$

where θ is the scattering angle and $\omega' = \omega\left(1 + \frac{\omega}{m_p}\,(1-\cos\theta)\right)^{-1}$ is the energy of the final photon. In the expression above we have included a form factor

$$F(t) = \frac{m_p^2 - 0.7\,t}{\left(m_p^2 - 0.25\,t\right)\left(1 - \dfrac{t}{(0.7\,{\rm GeV})^2}\right)^2} \tag{2.3}$$

that suppresses elastic scatterings with large momentum transfer. Going back to the frame with the nucleus at rest, we can express this cross section in terms of the fraction of energy ν lost by the incident proton:[3]

$$\frac{{\rm d}\sigma_{p\gamma\to p\gamma}}{{\rm d}\nu} = \frac{\pi\alpha^2\,|F(t)|^2}{m_p\,\omega}\left(\frac{1-\nu+\nu^2}{1-\nu} + \left(1 - \frac{m_p}{\omega}\,\frac{\nu}{1-\nu}\right)^2\right), \tag{2.4}$$

with $t = -2\omega\nu m_p$. Adding the contribution of all the equivalent photons we obtain

$$\frac{{\rm d}\sigma_{p{\rm N}\to p\gamma{\rm N}}}{{\rm d}\nu} = \int {\rm d}\omega\, \frac{{\rm d}N_\gamma}{{\rm d}\omega}\, \frac{{\rm d}\sigma_{p\gamma\to p\gamma}}{{\rm d}\nu}\,, \tag{2.5}$$

[3] Notice that ν and ω are kinematical variables defined in different reference frames.

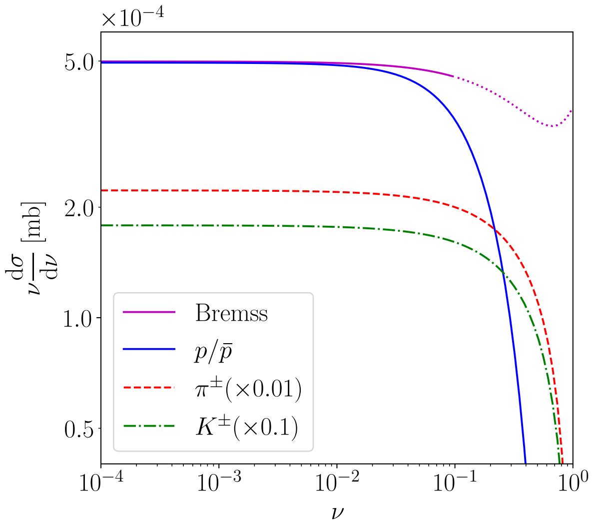

Figure 2. Bremsstrahlung cross section off a nitrogen nucleus for a point-like proton and our estimate obtained using the equivalent photon approximation for charged hadrons.

with $\omega_{\rm min} = \frac{m}{2}\,\frac{\nu}{1-\nu}$. We find that this cross section for bremsstrahlung (pN $\to p\gamma$N) obtained using inverse Compton scattering ($p\gamma \to p\gamma$, where the γ is an equivalent photon around the nitrogen nucleus) gives an excellent approximation to the explicit calculation (see [13] and references therein). In figure 2 we compare both cross sections for a 10^{10} GeV proton (the dependence with the energy of the projectile for $E > 1$ TeV is negligible). In the EPA (see eq. (2.1)) we have taken $b_{\rm max} = \pi/(\alpha\, m_e)$, whereas the bremsstrahlung cross section corresponds to a point-like proton (the form factor suppresses the differential cross section only at $\nu \geq 0.1$). An analogous calculation for charged mesons ($h = \pi, K$), with

$$\frac{{\rm d}\sigma_{h\gamma\to h\gamma}}{{\rm d}\nu} = \frac{\pi\alpha^2\,|F(t)|^2}{m_h\,\omega}\left(1 + \left(1 - \frac{m}{\omega}\,\frac{\nu}{1-\nu}\right)^2\right), \tag{2.6}$$

gives the cross sections also included in figure 2.

We can now estimate the collision of the projectile h with equivalent photons of higher energy, $\omega \geq 1$ GeV in the frame with h at rest. These are inelastic collisions ($\gamma h \to X$) where the hadron absorbs the photon and goes to a final state with pions [14]. In figure 3-left we plot our fit for such collisions; we include the first resonances plus

$$\sigma_{\gamma h}(s) = A_h\, s^{0.0808} + B_h\, s^{-0.4525}\,, \tag{2.7}$$

with $A_p = 0.069$, $B_p = 0.129$; $A_\pi = 0.044$, $B_\pi = 0.0734$; $A_K = 0.038$, $B_p = 0.059$ and $s = 2\omega m_h + m_h^2$. Adding the contribution of all the photons in the N cloud we obtain the total diffractive cross section in figure 3-right. In these EM processes 30% of the cross section comes from collisions with low-energy equivalent photons that take the incident projectile to a hadronic resonance: $\Delta(1232)$ to $\Delta(1950)$ for the proton, $\rho(770)$ to $a_2(1320)$ for pions, and $K^*(892)$ to $K_2^*(1430)$ for kaons. In this case, the final state will typically include an extra pion carrying a fraction $m_\pi/(m_\pi + m_h)$ of the incident energy, whereas in the remaining 70% of the cases the final state will include several pions.

JCAP07(2023)025

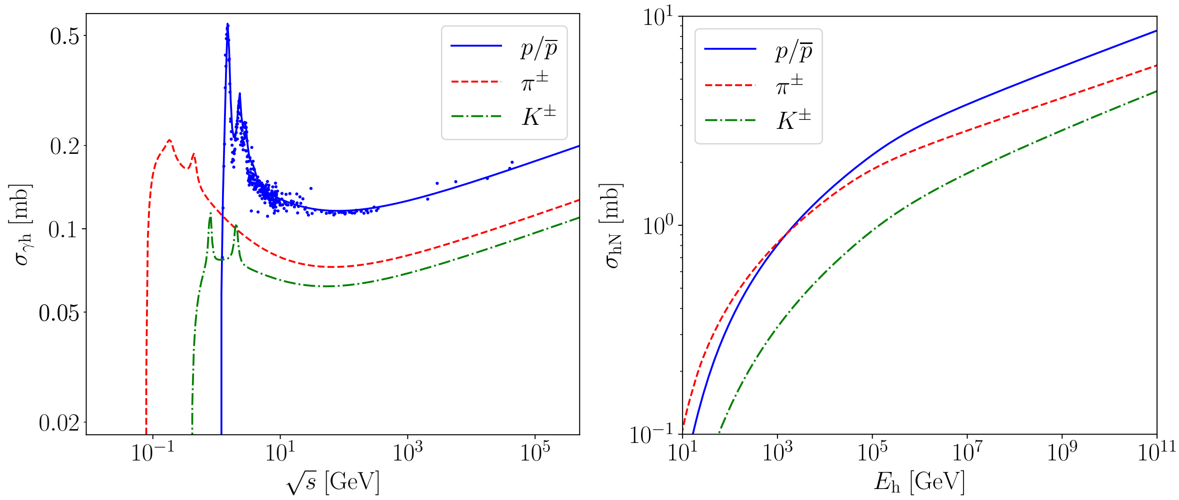

Figure 3. Cross section $\sigma_{\gamma h}$ and our estimate for the diffractive cross section $\sigma_{hN}^{\rm diff}$ in the EPA.

The EM diffractive cross section that we have obtained implies an interaction length (in g/cm^2) in nitrogen $\lambda_{hN}^{\rm diff} = m_{\rm N}/\sigma_{hN}^{\rm diff}$. In the air, if we take a 72% N plus 28% O composition,

$$\frac{1}{\lambda_{hN}^{\rm diff}} = \frac{0.72\,\sigma_{hN}^{\rm diff}}{m_{\rm N}} + \frac{0.28\,\sigma_{hO}^{\rm diff}}{m_{\rm O}}\,. \tag{2.8}$$

Since $\sigma_{hO}^{\rm diff}/\sigma_{hN}^{\rm diff} \approx (8/7)^2$, we obtain

$$\lambda_{h\,\rm air}^{\rm diff} \approx 0.96\,\frac{m_{\rm N}}{\sigma_{hN}^{\rm diff}}\,, \tag{2.9}$$

with a 69% probability for a hN collision and a 31% probability for a collision with O. These approximate relations hold for bremsstrahlung and pair production as well.

3 Pair production and photonuclear collisions

The two processes discussed in the previous section can be understood as the collision of the projectile with the photon cloud around the atmospheric nucleus. But we also have the opposite process, the collision of the equivalent photons carried by the charged hadron with the nucleus. Obviously, these collisions will only depend on the velocity (or the Lorentz factor $\gamma = E/m_h$) of h. In the frame with the nucleus at rest, their spectrum is given by

$$\frac{{\rm d}N_\gamma}{{\rm d}\omega} = \frac{\alpha\,b_{\rm min}}{\pi\,\gamma^2}\left(\omega\,b_{\rm min}\,K_0(x_{\rm min})^2 + 2\gamma\,K_1(x_{\rm min})\,K_0(x_{\rm min}) - \omega\,b_{\rm min}\,K_1(x_{\rm min})^2\right), \tag{3.1}$$

with $x_{\rm min} = \omega b_{\rm min}/\gamma$ and $b_{\rm min} = (0.17\,{\rm GeV})^{-1}$. As the equivalent photons propagate in the atmosphere they may create an e^+e^- pair or experience a photonuclear collision. Let us first discuss pair production [15].

At photon energies above 10 GeV the cross section to convert into a pair becomes constant,

$$\sigma_\gamma = \frac{7\,m_A}{9\,X_0}\,, \tag{3.2}$$

JCAP07(2023)025

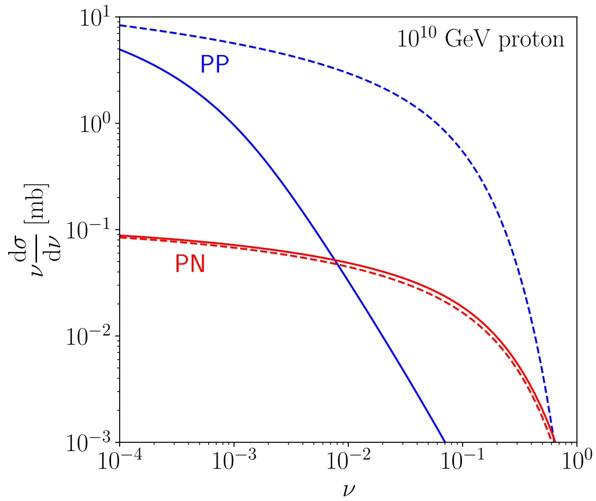

Figure 4. Pair production (PP) and photonuclear (PN) cross sections obtained using the equivalent photon approximation (dashes) and from an explicit calculation (solid).

where m_A is the mass of the nucleus in the medium and X_0 the radiation length. Including screening, collisions with electrons, and radiative corrections one has

$$X_0 = \frac{m_A}{4\alpha r_e^2 \left(Z^2 \left(\ln \frac{184}{Z^{1/3}} - f(Z) \right) + Z \ln \frac{1194}{Z^{2/3}} \right)}, \tag{3.3}$$

with

$$f(Z) = (\alpha Z)^2 \sum_{n=1}^{\infty} \frac{1}{n \left(n^2 + (\alpha Z)^2 \right)} . \tag{3.4}$$

In a nitrogen medium $\sigma_\gamma = 470$ mb and $X_0 = 38.4$ g/cm^2, whereas in the atmosphere the radiation length is a 4% shorter (see the discussion at the end of section 2). Including all the photons in the cloud, the differential cross section for a hadron h of energy E to loose a fraction ν of its energy by the conversion of one of these photons into an e^+e^- pair would be

$$\frac{d\sigma(hN \to he^+e^-N)}{d\nu} \equiv \frac{d\sigma_h}{d\nu} = E \frac{dN_\gamma}{d\omega} \sigma_\gamma . \tag{3.5}$$

In figure 4, we plot this result for a proton projectile (dashes) together with the result from an explicit calculation (solid) [13]. The EPA overestimates the pair production cross section; indeed, to neglect the off-shellness of these equivalent photons is not a good approximation when the final state has an invariant mass of order $2m_e$ [16]. For $E > 1$ TeV, this cross section is independent from the projectile energy. The differential cross section for pions and kaons can be readily obtained from

$$\left. \frac{d\sigma_h}{d\nu} \right|_{(\nu,E)} = r_h \left. \frac{d\sigma_p}{d\nu} \right|_{(r_h\nu,\, r_h^{-1}E)} \tag{3.6}$$

where $r_h \equiv m_h/m_p$,

Finally, there are the processes where the photons in the cloud around h experience a hadronic collision (radiative photonuclear collisions [17]). Assuming vector meson dominance, a photon carrying a fraction ν of the hadron's energy fluctuates into a $q\bar{q}$ pair; the pair forms a ρ (or a J/Ψ) meson that may then interact elastically ($\gamma N \to \rho N$) or inelastically with the nitrogen nucleus. In figure 4, we include the result for a 10^{10} proton projectile (the relation in eq. (3.6) for pions and kaons is also valid in this case) together with the explicit calculation of the cross section [18, 19]. We see that in this case the EPA gives an excellent agreement. We provide fits for all these ultra-peripheral processes in the next section.

4 AIRES simulations

AIRES includes the energy loss by ionization of charged hadrons, but not the radiative emissions considered in previous sections. These dominate over ionization at Lorentz factors above $\gamma_c \approx 2000$, i.e., at energies above 2 TeV for protons, 1 TeV for kaons and 300 GeV for pions. Our objective is then to modify the propagation of these high energy charged hadrons in an EAS.

In table 1, we provide the different interaction lengths in air for protons, pions and kaons at energies between 10^2 and 10^{11} GeV. The lengths $\lambda^h_{\rm BR}$ and $\lambda^h_{\rm PP}$ correspond to energy depositions $E_{\rm dep} > 0.1$ GeV or $\nu_{\rm min} = \frac{0.1\,{\rm GeV}}{E}$, whereas in photonuclear depositions we take

$$\frac{E_{\rm dep}}{\rm GeV} > \sqrt{\frac{E}{100\,{\rm GeV}}} \quad \text{or} \quad \nu_{\rm min} = 0.1\sqrt{\frac{\rm GeV}{E}}\,. \tag{4.1}$$

Up to an energy-dependent normalization, the approximate ν distribution in each process is the following. In a bremsstrahlung collision

$$f^{\pi}_{\rm BR}(\nu) = \frac{1}{\nu}\,(1-\nu)^{1.25}\,; \tag{4.2}$$

$$f^{K}_{\rm BR}(\nu) = \frac{1}{\nu}\,(1-1.2\,\nu)^{1.25}\,, \tag{4.3}$$

$$f^{p}_{\rm BR}(\nu) = \frac{1}{\nu}\,(1-1.2\,\nu)^{2.20}\,; \tag{4.4}$$

with $\nu \le 0.8$. In the emission of an e^+e^- pair by a pion projectile the ν distribution is given by

$$f^{\pi}_{\rm PP}(\nu) = \frac{1-\nu}{\nu^{1.18}\,(1+4571\,\nu^{2.64})}\,, \tag{4.5}$$

whereas for $h = p, K$

$$f^{h}_{\rm PP}(\nu) = \frac{m_h}{m_\pi}\,f^{\pi}_{\rm PP}(m_h\,\nu/m_\pi)\,. \tag{4.6}$$

Finally, in a photonuclear collision we obtain

$$f^{\pi}_{\rm PN}(\nu) = \frac{1-\nu^{0.22}}{\nu^{0.981}}\,, \tag{4.7}$$

with a negligible dependence on the energy of the projectile (other than the dependence in $\nu_{\rm min}$). The distribution for protons and kaons given also by the relation in (4.6).

The implementation of these processes in AIRES has been done in two steps: *(i)* we modify the mean free path (shortened by the new interactions) and find the relative frequency of each process, and *(ii)* we characterize the final state for these processes.

In bremsstrahlung and pair-production the final state includes a real photon or an e^+e^- pair with the ν-distributions given above. In our estimate we will take all the radiative emissions in the direction of the projectile, with equal energy for the two electrons in the pair.

JCAP07(2023)025

Energy [GeV]	$\lambda^p_{\rm had}$ [g/cm^2]	$\lambda^p_{\rm BR}$ [g/cm^2]	$\lambda^p_{\rm DIFF}$ [g/cm^2]	$\lambda^p_{\rm PP}$ [g/cm^2]	$\lambda^p_{\rm PH}$ [g/cm^2]
10^3	83.3	76.8×10^5	26.2×10^3	33.1×10^2	31.9×10^4
10^4	76.7	50.0×10^5	15.2×10^3	940	20.6×10^4
10^5	71.1	38.5×10^5	99.5×10^2	426	13.8×10^4
10^6	64.1	32.1×10^5	73.0×10^2	241	93.1×10^3
10^7	56.6	27.6×10^5	57.9×10^2	155	63.7×10^3
10^8	50.5	24.3×10^5	47.0×10^2	108	44.4×10^3
10^9	45.5	21.7×10^5	38.4×10^2	79.1	31.7×10^3
10^{10}	41.6	19.5×10^5	31.5×10^2	60.5	23.1×10^3
10^{11}	38.3	17.8×10^5	25.9×10^2	48.1	19.4×10^3
Energy [GeV]	$\lambda^\pi_{\rm had}$ [g/cm^2]	$\lambda^\pi_{\rm BR}$ [g/cm^2]	$\lambda^\pi_{\rm DIFF}$ [g/cm^2]	$\lambda^\pi_{\rm PP}$ [g/cm^2]	$\lambda^\pi_{\rm PH}$ [g/cm^2]
10^3	111	13.3×10^4	26.3×10^3	11.2×10^2	18.3×10^4
10^4	99.5	99.7×10^3	16.6×10^3	480	12.7×10^4
10^5	89.3	81.0×10^3	11.7×10^3	264	89.1×10^3
10^6	79.8	68.5×10^3	92.3×10^2	166	62.5×10^3
10^7	69.3	59.4×10^3	76.4×10^2	114	44.3×10^3
10^8	59.3	52.5×10^3	63.9×10^2	83.3	31.8×10^3
10^9	52.2	46.8×10^3	53.6×10^2	63.4	23.3×10^3
10^{10}	46.9	42.5×10^3	44.9×10^2	49.7	17.4×10^3
10^{11}	42.9	38.7×10^3	37.5×10^2	40.4	14.7×10^3
Energy [GeV]	$\lambda^K_{\rm had}$ [g/cm^2]	$\lambda^K_{\rm BR}$ [g/cm^2]	$\lambda^K_{\rm DIFF}$ [g/cm^2]	$\lambda^K_{\rm PP}$ [g/cm^2]	$\lambda^K_{\rm PH}$ [g/cm^2]
10^3	125	18.9×10^5	60.7×10^3	21.6×10^2	25.6×10^4
10^4	115	13.1×10^5	34.1×10^3	730	17.1×10^4
10^5	103	10.3×10^5	21.8×10^3	357	11.7×10^4
10^6	89.9	86.9×10^4	15.6×10^3	211	80.0×10^3
10^7	76.7	75.1×10^4	12.0×10^3	139	55.6×10^3
10^8	65.1	66.0×10^4	94.8×10^2	98.4	39.2×10^3
10^9	57.0	59.1×10^4	76.0×10^2	73.2	28.3×10^3
10^{10}	51.1	53.4×10^4	61.4×10^2	56.5	20.8×10^3
10^{11}	46.6	48.7×10^4	49.9×10^2	45.3	17.5×10^3

Table 1. Interaction length in air for the different processes, projectiles and energies.

In a diffractive collision the energy of the equivalent photon around the nucleus is sampled. We will assume a final state with a leading hadron (a nucleon or a K meson in proton and $K^\pm$ collisions, respectively) plus only pions. In particular, for an interaction of $E_\gamma < 2\,$GeV the final-state will just include one or two extra pions, whereas at higher photon energies we take a multiplicity

$$n_\pi = \text{Max}\,[\,2,\ 2.3\log_{10}(E_\gamma/\text{GeV})\,]\,. \tag{4.8}$$

In these multi-pion diffractive collisions the leading baryon is a proton 2.2 times more frequently than a neutron, whereas pions appear in the three flavors with similar frequency. We assume equipartition of the initial energy among the final particles according to

$$E_i = \frac{m_i}{\sum_j m_j} E_h. \tag{4.9}$$

JCAP07(2023)025

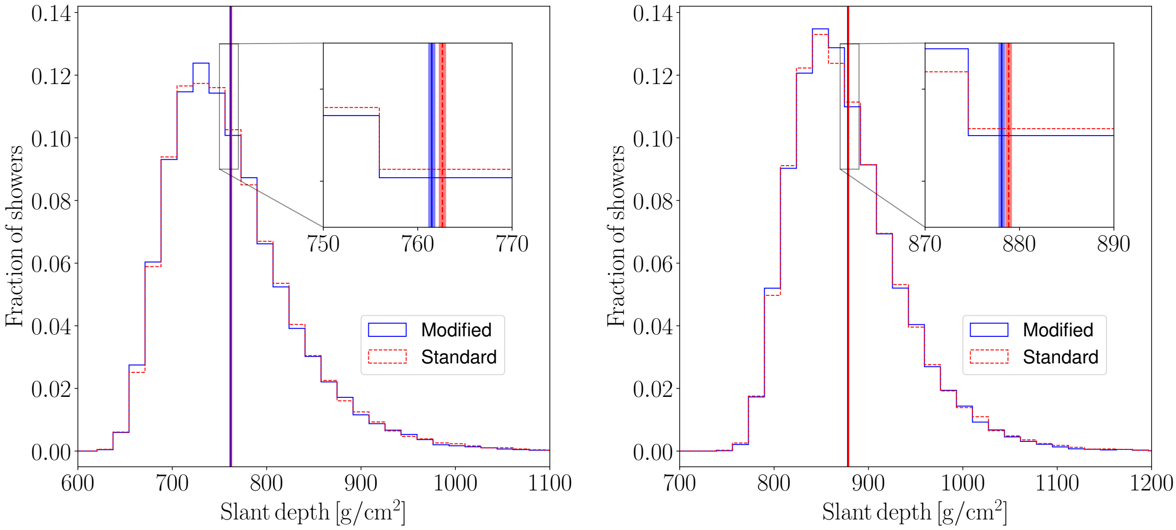

Figure 5. Distribution of $X_{\rm max}$ for 40.000 proton primaries of $E = 10^9$, 10^{11} GeV (the bands indicate the statistical uncertainty).

E [GeV]	10^9	10^{10}	10^{11}
$\langle X_{\rm max}^{\rm mod}\rangle$ [g/cm^2]	761.4	819.5	878.1
$\langle X_{\rm max}^{\rm st}\rangle$ [g/cm^2]	762.6	820.4	878.9
$\Delta X_{\rm max}^{\rm mod}$ [g/cm^2]	66.3	62.3	58.9
$\Delta X_{\rm max}^{\rm st}$ [g/cm^2]	67.3	62.7	59.8

Table 2. Average value of $X_{\rm max}$ and $\Delta X_{\rm max}$ for 40.000 proton primaries of each energy.

Finally, in a radiative photonuclear interaction the photon is sampled and treated as a real photon that is processed with the Monte Carlo simulator SIBYLL [20].

Let us discuss the effect of these EM processes by comparing the results in *modified* runs of AIRES that include these EM processes with the results in *standard* runs. We will use the SIBYLL option and 0.1 GeV as the minimum photon energy, with a relative thinning of 10^{-4}. Each run contains 40.000 proton events from a zenith inclination $\theta_z = 70°$. In figure 5, we plot the distribution of the shower maximum for primaries of $E = 10^9$, 10^{11} GeV. We observe that the inclusion of the EM processes increases the fraction of events with a small value of $X_{\rm max}$, but the effect on $\langle X_{\rm max}\rangle$ is just a reduction of 1.2 g/cm^2 at 10^9 GeV or of 0.8 g/cm^2 at 10^{11} GeV, with a statistical uncertainty of 0.3 g/cm^2. In table 2, we provide $\langle X_{\rm max}\rangle$ together with the value of the dispersion $\Delta X_{\rm max}$, which in the modified run decreases by a 0.6% at 10^{10} GeV.

The shift in $\langle X_{\rm max}\rangle$ implies a small reduction in the average number of particles at a given slant depth after $X_{\rm max}$, as we see figure 6. The effects are better understood if we center each shower at $X_{\rm max}$ and express the results in terms of the shower age s [21],

$$s = \frac{3X}{X + 2X_{\rm max}}\,, \tag{4.10}$$

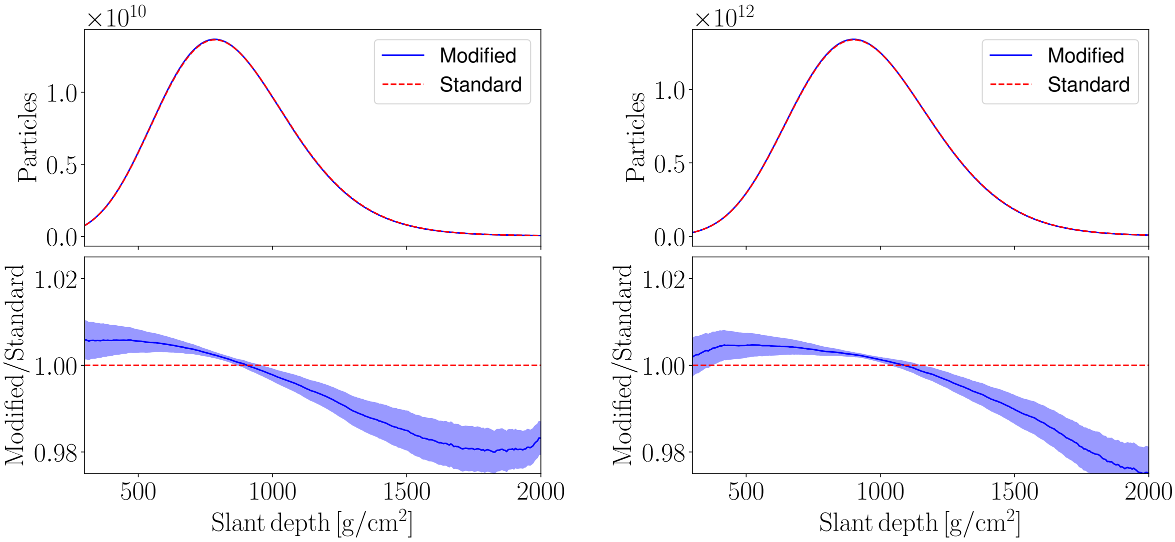

Figure 6. Total number of particles at different slant depths and relative difference between the standard and modified runs for 10^9 GeV (left) and 10^{11} GeV (right).

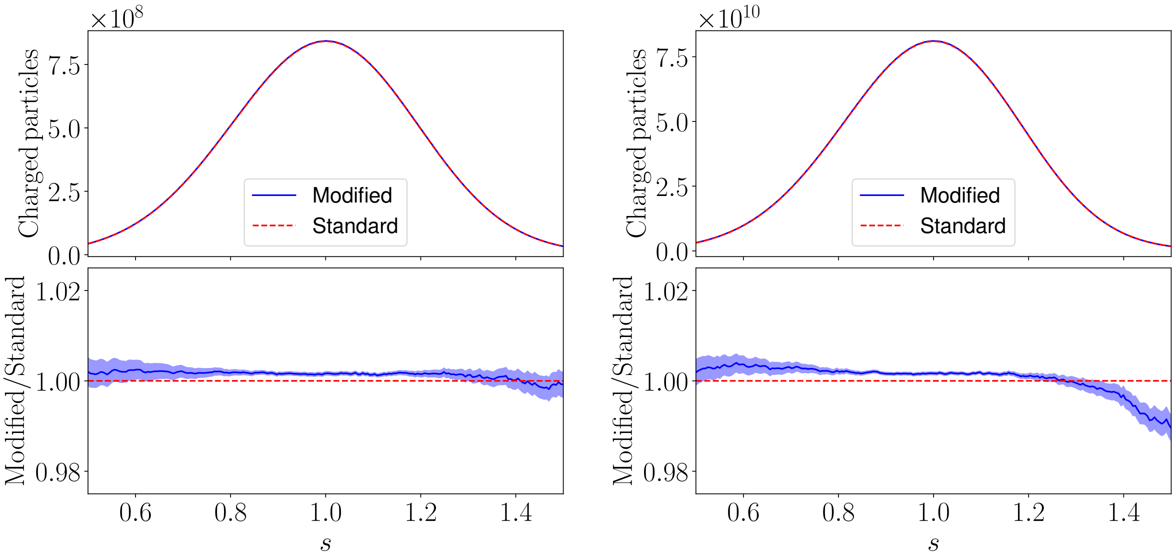

Figure 7. Number of charged particles in terms of the shower age s as defined in eq. (4.10) for 10^9 GeV (left) and 10^{11} GeV (right).

with $s = 1$ at $X = X_{\max}$ (see also [22] for a more accurate definition of the shower age). In figure 7, we plot the number of charged particles for different values of s. We obtain that the effect of the new interactions is an increase below 1% in the signal when the shower is young ($s \leq 0.6$) and at the shower maximum, together with a decrease when the shower is old ($s \geq 1.4$). Such variation, although not observable experimentally, seems clear at the energies considered.

The effect on the number of muons is illustrated in figure 8. We find that young showers include more muons (the excess is below 1%) than in the average standard run, but as the shower develops the number of muons becomes 1% smaller. As a consequence, the showers

JCAP07(2023)025

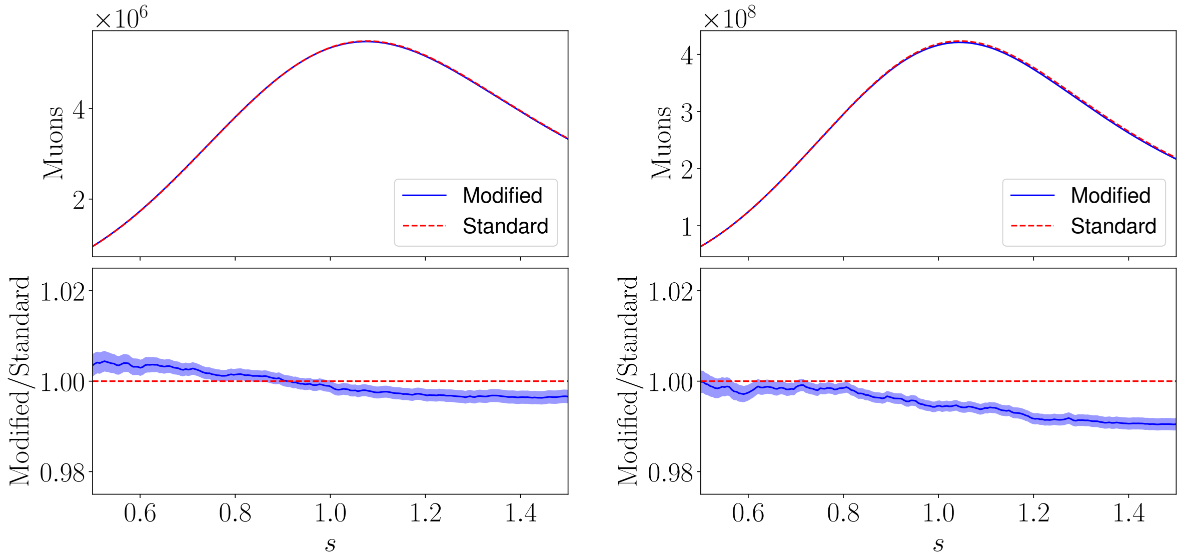

Figure 8. Number of muons in terms of the shower age s as defined in eq. (4.10) for two different energies, 10^9 GeV (left) and 10^{11} GeV (right).

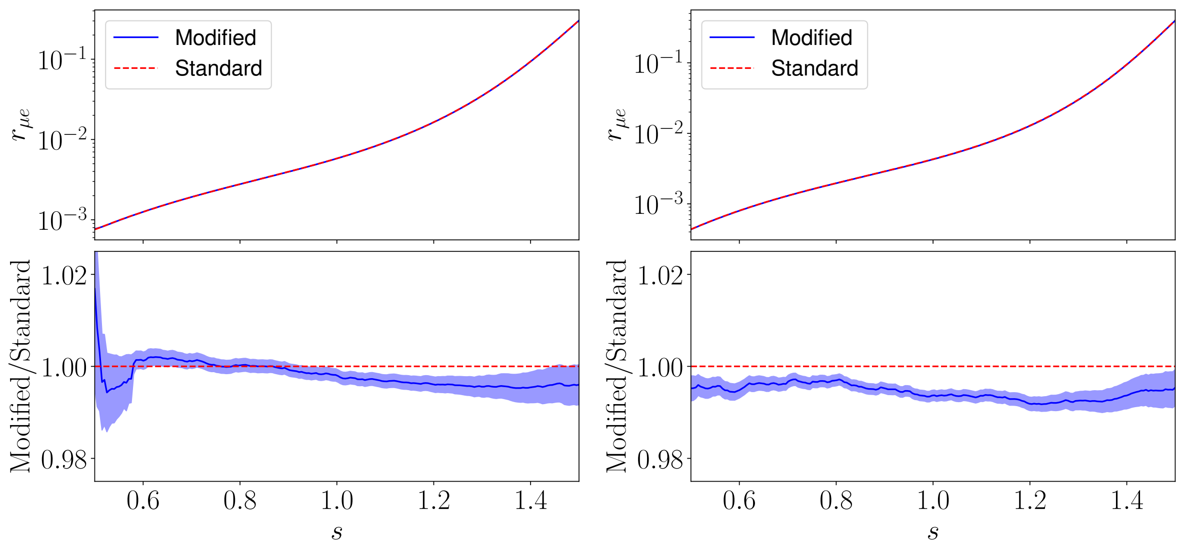

Figure 9. Muon to EM ratio $r_{\mu e}$ in terms of the shower age.

evolve from $X_{\max}$ with a slightly poorer muon-to-electron ratio. This can be expressed in terms of $r_{\mu e}$ [23], the ratio between the number of muons and the energy of $(e^+ + e^- + \gamma)$ in units of 500 MeV:

$$r_{\mu e} \equiv \frac{n_\mu}{E_{e+\gamma}/(0.5\,\text{GeV})}\,. \tag{4.11}$$

We plot this observable in figure 9, where we appreciate a 1% reduction at $s > 1$ due to the new EM interactions.

5 Summary and discussion

The EM interactions of charged hadrons at very high energies are not included in current EAS simulators like AIRES or CORSIKA. At these energies, the projectile may *break* when crossing the EM field of an air nucleus at relatively large transverse distances (a diffractive collision), or it may radiate a real photon (bremsstrahlung), or it may radiate a virtual photon that converts into a pair (e^+e^- emission) or a rho meson (photonuclear collision). These ultra-peripheral processes have a longer interaction length than the hadronic ones, but we think that a precise estimate of their effect on EASs was long due. Here we have parametrized them and have then used AIRES to find the changes in $X_{\rm max}$ and in the muon or electron abundances at different slant depths that they introduce. We obtain 1% corrections that, given the precision and the reduced statistics in EAS experiments, are far from being observable.

Despite the reduced size of these effects, they are significant (non-zero) and consistent. First of all, there is a slight excess (around 0.3%) in the number of particles near $X_{\rm max}$; this excess becomes a deficit when the shower is old. Second, the shower maximum is slightly shifted: the new interactions reduce in a few g/cm^2 the value of $X_{\rm max}$. This implies that at a given slant depth the showers are now a bit older. Third, old showers have less muons and a 1% smaller muon-to-EM ratio. These effects just reflect *(i)* that the average shower develops *faster* due to the new collisions, and *(ii)* that the ratio of photons to charged pions introduced by these EM processes is larger than in hadronic collisions.

Our results underline the consistency and the stability of current simulators under the type of processes considered. Despite their sizeable cross section, ultra-peripheral collisions are events of low inelasticity, and their inclusion in these simulators would improve their accuracy in just a 1%.

Acknowledgments

This work was partially supported by the Spanish Ministry of Science, Innovation and Universities (PID2019-107844GB-C21/AEI/10.13039/501100011033), by Consejería de Universidad, Investigación e Innovación de la Junta de Andalucía/FEDER (P18-FR-5057), Consejo Nacional de Investigaciones Científicas y Técnicas (CONICET) of Argentina, and Agencia Nacional de Promoción Científica y Tecnológica (ANPCyT) of Argentina.

References

[1] T.K. Gaisser, *Cosmic rays and particle physics*, Cambridge University Press (1990) [INSPIRE].

[2] P. Lipari, *Lepton spectra in the earth's atmosphere*, *Astropart. Phys.* **1** (1993) 195 [INSPIRE].

[3] Pierre Auger collaboration, *The Pierre Auger Observatory Upgrade — Preliminary Design Report*, arXiv:1604.03637 [INSPIRE].

[4] R. Ulrich et al., *Sensitivity of Extensive Air Showers to Features of Hadronic Interactions at Ultra-High Energies*, arXiv:0906.0418 [INSPIRE].

[5] S.J. Sciutto, *AIRES: A system for air shower simulations*, astro-ph/9911331 [DOI:10.13140/RG.2.2.12566.40002] [http://aires.fisica.unlp.edu.ar] [INSPIRE].

[6] R. Engel et al., *Towards a Next Generation of CORSIKA: A Framework for the Simulation of Particle Cascades in Astroparticle Physics*, *Comput. Softw. Big Sci.* **3** (2019) 2 [arXiv:1808.08226] [INSPIRE].

[7] D. Heck et al., *CORSIKA: A Monte Carlo code to simulate extensive air showers*, FZKA-6019 (1998) [INSPIRE].

[8] V. Guzey and M. Strikman, *Proton-nucleus scattering and cross section fluctuations at RHIC and LHC*, Phys. Lett. B **633** (2006) 245 [hep-ph/0505088] [INSPIRE].

[9] K. Greisen, *End to the cosmic ray spectrum?*, Phys. Rev. Lett. **16** (1966) 748 [INSPIRE].

[10] G.T. Zatsepin and V.A. Kuzmin, *Upper limit of the spectrum of cosmic rays*, *JETP Lett.* **4** (1966) 78 [INSPIRE].

[11] E. Fermi, *On the theory of collisions between atoms and electrically charged particles*, Nuovo Cim. **2** (1925) 143 [hep-th/0205086] [INSPIRE].

[12] C.A. Bertulani, S.R. Klein and J. Nystrand, *Physics of ultra-peripheral nuclear collisions*, Ann. Rev. Nucl. Part. Sci. **55** (2005) 271 [nucl-ex/0502005] [INSPIRE].

[13] D.E. Groom, N.V. Mokhov and S.I. Striganov, *Muon stopping power and range tables 10 MeV–100 TeV*, Atom. Data Nucl. Data Tabl. **78** (2001) 183 [INSPIRE].

[14] A. Mucke et al., *SOPHIA: Monte Carlo simulations of photohadronic processes in astrophysics*, Comput. Phys. Commun. **124** (2000) 290 [astro-ph/9903478] [INSPIRE].

[15] S.R. Klein, *e^+e^- pair production from 10 GeV to 10 ZeV*, Radiat. Phys. Chem. **75** (2006) 696 [hep-ex/0402028] [INSPIRE].

[16] V.M. Budnev, I.F. Ginzburg, G.V. Meledin and V.G. Serbo, *The Two photon particle production mechanism. Physical problems. Applications. Equivalent photon approximation*, Phys. Rept. **15** (1975) 181 [INSPIRE].

[17] G.A. Schuler and T. Sjostrand, *Towards a complete description of high-energy photoproduction*, Nucl. Phys. B **407** (1993) 539 [INSPIRE].

[18] V.V. Borog and A.A. Petrukhin, *The Cross-Section of the Nuclear Interaction of High-Energy Muons*, in the proceedings of the *14th International Cosmic Ray Conference*, (1975) [INSPIRE].

[19] R. Brun, R. Hagelberg, M. Hansroul and J.C. Lassalle, *Geant: Simulation Program for Particle Physics Experiments. User Guide and Reference Manual*, CERN-DD-78-2-REV (1978) [INSPIRE].

[20] F. Riehn et al., *Hadronic interaction model Sibyll 2.3d and extensive air showers*, Phys. Rev. D **102** (2020) 063002 [arXiv:1912.03300] [INSPIRE].

[21] D. Gora et al., *Universal lateral distribution of energy deposit in air showers and its application to shower reconstruction*, Astropart. Phys. **24** (2006) 484 [astro-ph/0505371] [INSPIRE].

[22] P. Lipari, *The Concepts of 'Age' and 'Universality' in Cosmic Ray Showers*, Phys. Rev. D **79** (2009) 063001 [arXiv:0809.0190] [INSPIRE].

[23] C.A. García Canal, J.I. Illana, M. Masip and S.J. Sciutto, *A new observable in extensive air showers*, Astropart. Phys. **85** (2016) 50 [arXiv:1609.04941] [INSPIRE].

JCAP07(2023)025